ELSEVIER

Catalysis Today 40 (1998) 47–57

CATALYSIS TODAY

Elemental sulfur production during the regeneration of iron oxide high-temperature desulfurization sorbent

J.D. White, F.R. Groves Jr., D.P. Harrison*

Department of Chemical Engineering, Louisiana State University, Baton Rouge, Louisiana 70803, USA

Abstract

The production of elemental sulfur instead of SO_2 during the regeneration of high temperature desulfurization sorbents will improve the efficiency of advanced power generation processes such as the integrated gasification combined cycle (IGCC). While much research is directed at developing zinc-based sorbents because of the favorable thermodynamics of the ZnO–H_2S reaction, SO_2 is the inevitable product from ZnS regeneration. Iron-based sorbents, although less efficient for H_2S removal, permit significant amounts of elemental sulfur to be formed during regeneration. A laboratory-scale fixed-bed reactor has been used to study the regeneration of FeS in steam-oxygen mixtures. The experimental results are interpreted on the basis of four simultaneous reactions. Oxygen reacts rapidly with FeS to produce SO_2 and Fe_2O_3. Steam reacts to give Fe_3O_4 and H_2S. Elemental sulfur is formed by the reaction between H_2S and SO_2, and additional O_2 is consumed in converting Fe_3O_4 to Fe_2O_3. The maximum yield of elemental sulfur, approximately 75% of theoretical, was achieved using a large H_2O-to-O_2 ratio (200-to-1) at the lowest feasible regeneration temperature (600°C), and using a small regeneration gas feed rate. © 1998 Elsevier Science B.V.

1. Introduction

Although low temperature scrubbing technology for removing H_2S from fuel gas is well developed [1], there are potential advantages to be gained from high temperature desulfurization, and a great deal of research has been carried out in the last 25 years to develop a desulfurization process which can operate in the 400°C–800°C range. For example, the efficiency of advanced power generation processes based on the integrated gasification combined cycle (IGCC) can be increased significantly; coal-to-electricity efficiencies of approximately 50% are possible with high temperature desulfurization [2].

Much of the recent high temperature desulfurization research in the United States has concentrated on zinc-based sorbents such as zinc ferrite ($ZnFe_2O_4$) [3,4] and zinc titanate ($ZnO{\cdot}XTiO_2$) [5,6] because of the highly favorable thermodynamics of the ZnO–H_2S reaction. Zinc-based sorbent research has progressed to the point that laboratory tests consisting of at least 100 sulfidation–regeneration cycles have been completed [7], and two clean coal demonstration projects utilizing high temperature desulfurization are in early test phases [8]. Many of the problems with zinc-based sorbents are associated with the regeneration phase. The reaction between ZnS and O_2 is highly exothermic, which complicates reactor temperature control and may hasten sorbent deterioration. $ZnSO_4$ is stable and combinations of high temperature and low O_2 and

*Corresponding author.

PII S0920-5861(97)00120-X

SO_2 pressures are required to prevent sulfate formation. Sulfur is liberated during regeneration as SO_2 and additional processing steps are required to prevent the discharge of SO_2 to the atmosphere [9].

Although iron oxide is also capable of reacting with H_2S at high temperatures, the thermodynamics are less favorable than for the ZnO–H_2S reaction. Little research on iron-based sorbents has been carried out in the United States in the last twenty years. However, research is still active in Japan and The Netherlands [10]. In spite of poorer desulfurization performance, iron-based sorbents may be superior in the regeneration portion of the cycle. Direct formation of significant amounts of elemental sulfur has been reported when FeS was regenerated in an H_2O–O_2 atmosphere [11]. Partial oxidation to elemental sulfur is less exothermic, and separation can be achieved by condensation. Elemental sulfur has a market value and can be relatively easily and safely stored and transported. This study examined the formation of elemental sulfur during regeneration of FeS as a function of temperature, regeneration feed gas composition, and space velocity.

2. Experimental

A diagram of the fixed-bed reactor system is shown in Fig. 1. The flow rates of air and nitrogen were controlled by mass flow controllers. Water was added from a high pressure syringe pump, and feed lines were heat traced to insure vaporization and to preheat the combined reactor feed. Feed gas entered near the top of the reactor and flowed downward through the packed bed which was held in an insert inside the stainless steel pressure vessel. High temperature O-rings formed a seal between the insert and pressure vessel to prevent gas by-passing. The packed bed was supported by a porous quartz disk resting on "dimples" machined into the reactor insert. A layer of quartz wool was added between the porous disk and sorbent. All wetted steel surfaces were Alonized to minimize interaction between metal and sulfur gases.

Product gases exited from the bottom of the reactor and entered the analytical system shown in Fig. 2. The product gas was split into two streams, with one portion flowing through a capillary flow restrictor into

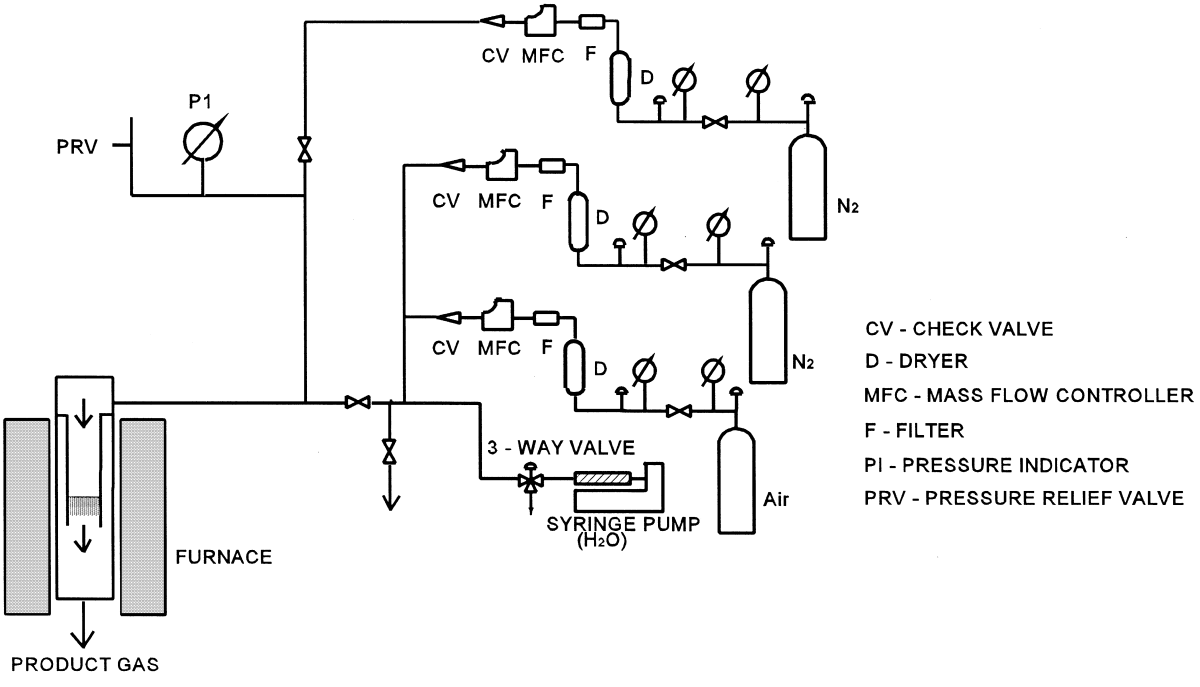

Fig. 1. The fixed-bed reactor system.

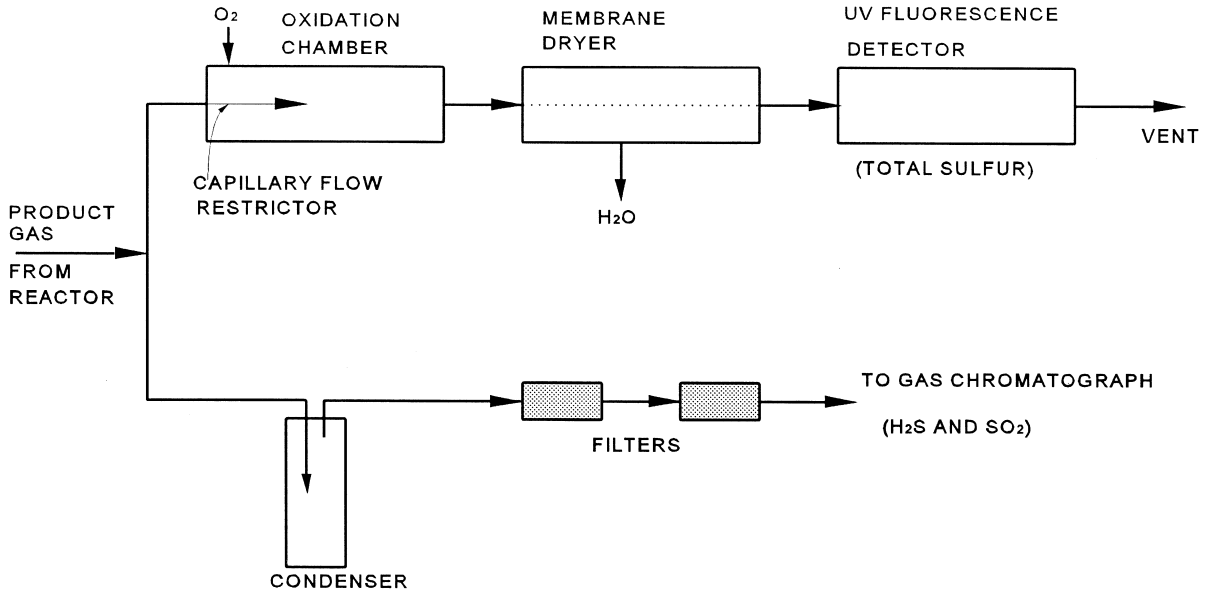

Fig. 2. System used for product gas analysis.

an oxidation chamber operated at 1050°C where all sulfur compounds were converted to SO_2. Excess H_2O was removed using a membrane dryer and total sulfur concentration was determined using a calibrated UV-fluorescence detector. Flow through this part of the analytical system was determined by the reactor pressure and the resistance of the capillary restrictor; frequent recalibration was necessary due to changing resistance of the restrictor caused by carryover of particles from the reactor. It was necessary to keep the temperature of the product gas above the condensation temperature of the elemental sulfur until it entered the oxidation chamber.

The remainder of the product gas entered the bottom part of the analytical system and passed through a condenser and series of filters where elemental sulfur was separated from the permanent gases. H_2S and SO_2 concentrations were then determined by gas chromatography. Although this analytical technique involved the determination of elemental sulfur by difference (total sulfur$-H_2S-SO_2$), it provided reasonable accuracy when the concentration of elemental sulfur was sufficiently large.

Reaction conditions associated with each of the experimental runs described in this paper are presented in Table 1. Pressure was constant at 4.4 atm while temperature was varied between 550 and 700°C. The regeneration feed gas contained from 0 to 1.5% O_2, 0 to 52% H_2O and balance N_2. In runs in which the feed gas contained both H_2O and O_2, the H_2O/O_2 ratio varied from 6.7 to 200. The sorbent bed consisted of a physical mixture of FeS and Al_2O_3, with the quantity of FeS varied in relation to the feed gas flow rate and O_2 content to insure complete regeneration in a reasonable time. The FeS, from Strem Chemicals, was 99.2±0.1% pure with a particle size range 60–200 mesh. The Al_2O_3, type F-20 from Sigma, had a particle size range 80–200 mesh and was added to minimize sintering. Volumetric feed rate was varied between 300 and 600 sccm to study the effect of residence time.

3. Results

With O_2 as the only reactive component in the feed gas (run FeS-11), the regeneration reaction is given by

$$2FeS(s) + \frac{7}{2}O_2(g) \rightarrow Fe_2O_3(s) + 2SO_2(g) \qquad (R1)$$

SO_2 and total sulfur concentrations in the product gas are equal. Experimental results from run FeS-11,

Table 1
Reaction conditions for FeS regeneration tests

Run	FeS-04	FeS-11	FeS-14	FeS-16	FeS-19	FeS-22	FeS-25	FeS-26
Sorbent Mass (g)								
Fes	1.73	3.27	3.22	3.21	0.83	0.83	0.50	0.83
Al_2O_3	3.04	3.29	3.21	3.27	3.28	3.28	3.80	3.29
Temperature (°C)	550	600	700	700	700	600	600	600
Pressure (atm)	4.4	4.4	4.4	4.4	4.4	4.4	4.4	4.4
Feed Gas Composition (mol%)								
O_2	0.5	1.5	0	1.5	0.25	0.25	0.26	0.25
H_2O	23.3	0	10.0	10.0	20.0	20.0	52.0	20.0
N_2	76.2	98.5	90.0	88.5	79.75	79.75	47.74	79.75
H_2O/O_2	47	–	–	6.7	80	80	200	80
Feed Gas Rate (sccm)	300	600	600	600	300	300	435	600

expressed as mol fraction SO_2 in the product gas as a function of dimensionless time, are shown in Fig. 3. Dimensionless time, t^*, is defined as follows

$$t^* = \frac{\frac{Q}{22{,}400} y_{O_2} t}{1.75 n_{FeS_i}} \quad (1)$$

where Q is the total volumetric feed rate (sccm), y_{O_2} is the mol fraction of O_2 in the feed gas, t is the dimensional time (min), n_{FeS_i} is the initial change of FeS (mol), 22,400 is the volume occupied by one mol of ideal gas at standard conditions, and 1.75 is the ratio of the stoichiometric coefficients of O_2 and FeS. $t^*=1$ would correspond to complete FeS regeneration and complete conversion of the gaseous reactant if the global reaction rate was infinitely fast. After a brief delay at the beginning of the run, the SO_2 concentration increased quickly to about 0.0085 mol fraction and was approximately constant until regeneration neared completion. The FeS–O_2 reaction was quite rapid as indicated by the steepness of the SO_2 concentration decrease near the end of the run, and the facts that the "steady-state" SO_2 concentration was near the stoichiometric value corresponding to complete O_2 consumption (indicated by the dashed horizontal line) and that the reaction was almost complete at $t^*=1.0$.

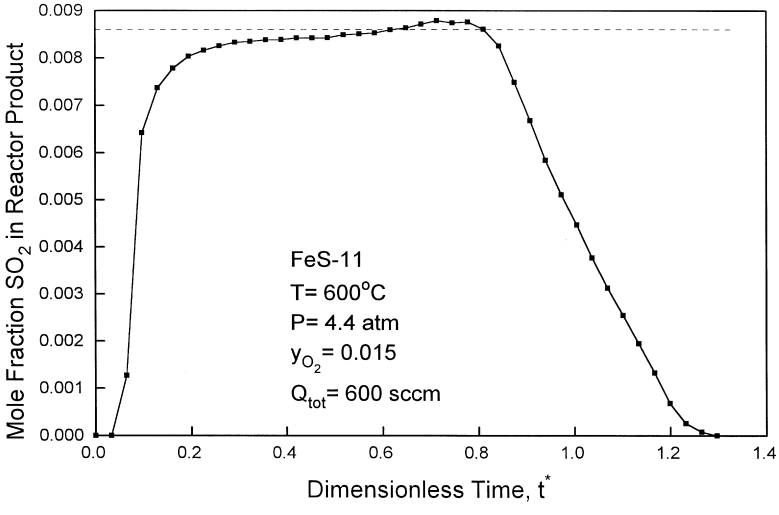

Fig. 3. SO_2 content of the product gas during oxygen regeneration: run FeS-11.

When the feed gas contained only H_2O, all sulfur was converted to H_2S, and the regeneration reaction is

$$3FeS(s) + 4H_2O(g) \rightarrow Fe_3O_4(s) + 3H_2S(g) + H_2(g) \quad \text{(R2)}$$

Experimental results from run FeS-14 are shown in Fig. 4. The "steady-state" H_2S mol fraction of 0.0013 was only about 1.7% of the stoichiometric maximum corresponding to reaction (R2), but was quite near the equilibrium value. Regeneration was only about 12% complete when the run was terminated after eight dimensionless time increments. Dimensionless time is again defined by Eq. (1) except that y_{H_2O} is used in place of y_{O_2} and 0.75 is substituted for 1.75.

In the presence of O_2 and H_2O, two additional reactions are believed to be important. Elemental sulfur is formed via the Claus reaction

$$SO_2(g) + 2H_2S(g) \rightarrow 2H_2O(g) + \frac{3}{2}S_2(g) \quad \text{(R3)}$$

Also, additional O_2 is consumed by

$$2Fe_3O_4(s) + \frac{1}{2}O_2(g) \rightarrow 3Fe_2O_3(s) \quad \text{(R4)}$$

The formation of elemental sulfur depends on the relative quantities of SO_2 and H_2S, and the position within the sorbent bed where they are formed. There must be sufficient H_2S–SO_2 contact time for the Claus reaction to occur. While other reaction such as the decomposition of H_2S may occur, the four reactions listed above are thought to be of primary importance.

The above interpretation is not consistent with generally accepted thermodynamics which shows that the Claus reaction equilibrium is unfavorable at the experimental conditions. However, the formation of significant amounts of elemental sulfur is certain. Other researchers, including Bennett and Meisen [12] and McMichael and Gangwal [13], have also reported elemental sulfur yields which exceed thermodynamic maxima under somewhat similar conditions. Bennett and Meisen concluded that the likely cause of the discrepancy was inaccurate thermodynamic data, most likely associated with elemental sulfur.

Results from run FeS-22 in which the feed gas containd both H_2O and O_2 in a 80-to-1 ratio are shown in Fig. 5. The mol fractions of SO_2, H_2S, and total sulfur (as S) in the product gas are plotted versus dimensional time. Dimensional time is used since dimensionless time cannot be clearly defined when multiple reactions occur simultaneously. Both the total sulfur and H_2S concentrations increased rapidly with the total sulfur approaching a maximum of 0.0025 mol fraction after 0.9 h and the H_2S maximum of 0.00065 mol fraction occurring after 1.7 h. SO_2 concentration

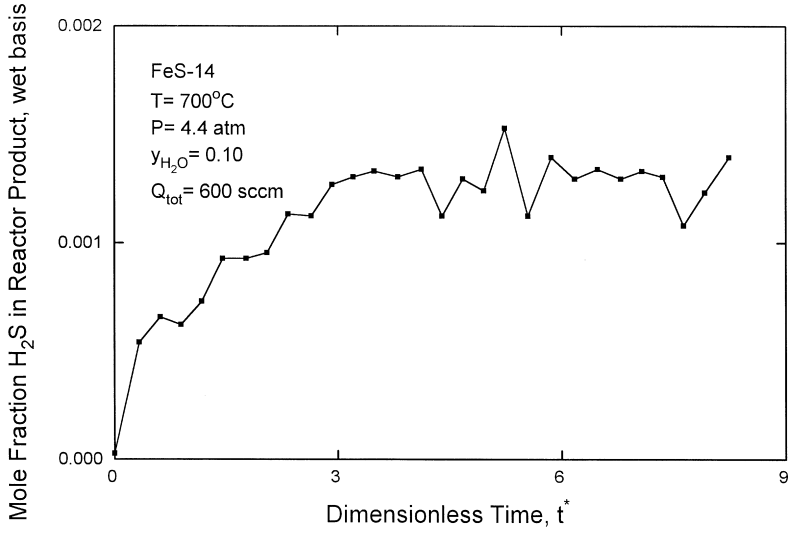

Fig. 4. H_2S content of the product gas during steam regeneration: run FeS-14.

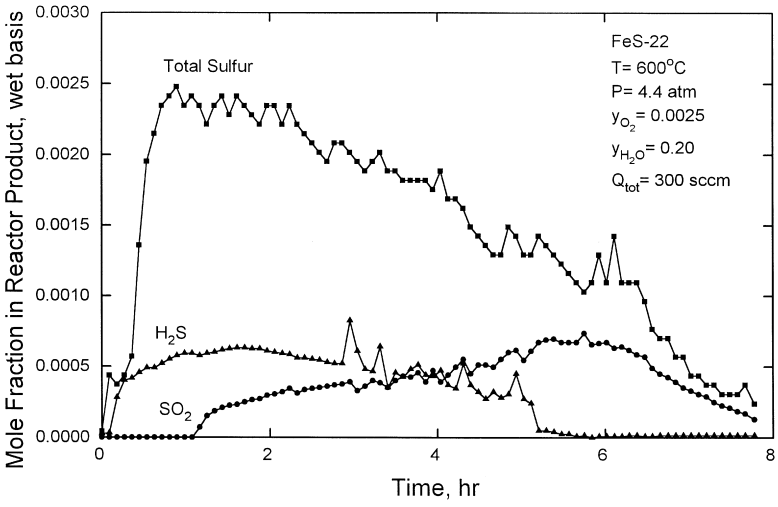

Fig. 5. Concentrations of sulfur species during steam-oxygen regeneration: run FeS-22.

was effectively zero during the first hour and then gradually increased to a maximum of 0.00072 at six hours. After reaching their maxima, the concentrations of all species gradually decreased with the H_2S mol fraction approaching zero after 5.1 h and the total sulfur and SO_2 mol fractions approaching zero at about eight hours.

Numerical integration of the concentration-time data was used to determine the cumulative amount of each sulfur species, as well as to provide a check on the sulfur material balance. Results of the numerical integration of run FeS-22 data are shown in Fig. 6. Cumulative production of H_2S, H_2S+SO_2, and total sulfur, all expressed as a fraction of theoretical sulfur associated with the initial FeS charge, are plotted versus reaction time. The brief time delay is again evident. The amount of H_2S gradually increased to account for about 21% of the total sulfur after 5.1 h after which no more H_2S was produced. The H_2S and H_2S+SO_2 curves coincide for the first hour when no

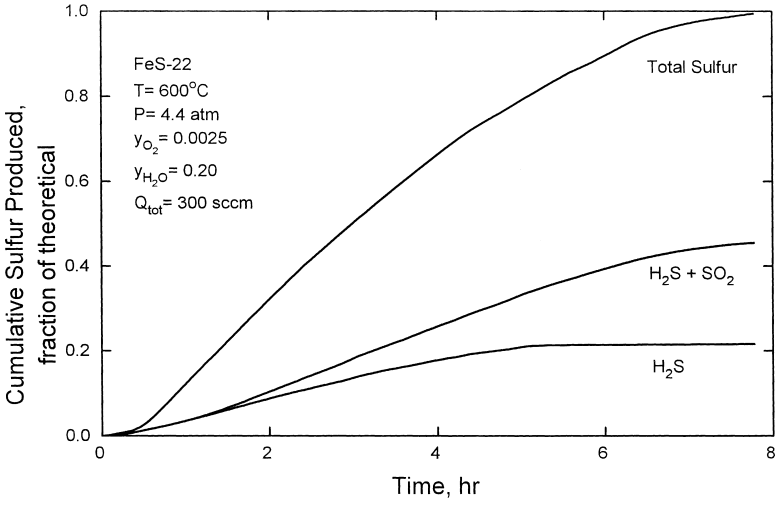

Fig. 6. Cumulative production of elemental sulfur, H_2S and SO_2 during steam–oxygen regeneration: run FeS-22.

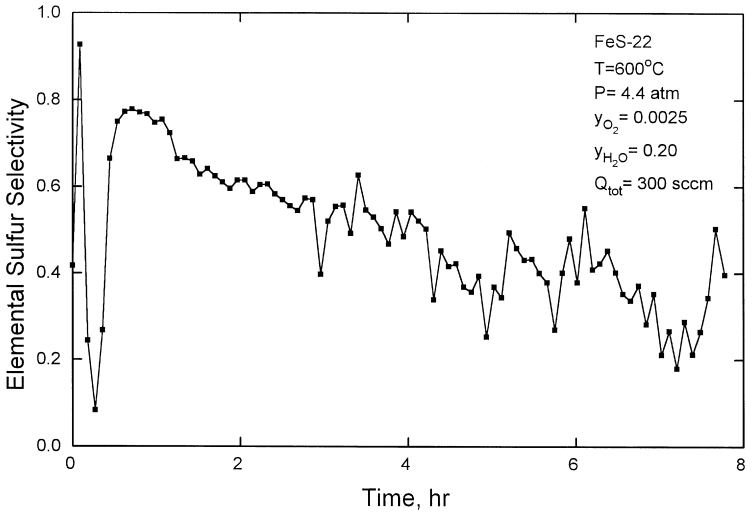

Fig. 7. Instantaneous selectivity to elemental sulfur: run FeS-22.

SO_2 was produced. Thereafter, the curves diverged and the cumulative production of SO_2 was 24% of theoretical to give the cumulative production of H_2S+SO_2 equal to 45% of theoretical. The overall sulfur balance in this run was quite good as the cumulative production of total sulfur was 99% of theoretical. Thus, about 55% of the sulfur was liberated in elemental form.

The instantaneous selectivity to elemental sulfur in run FeS-22 is shown in Fig. 7. Selectivity is defined by

$$S(t) = \frac{\text{Total Sulfur} - (SO_2 + H_2S)}{\text{Total Sulfur}} \quad (2)$$

Although there is significant scatter in the results, particularly near the beginning and end of the reaction where SO_2+H_2S concentrations are approximately equal to total sulfur concentration, there is a clear trend to the data. Near the beginning, about 80% of the sulfur was released in elemental form. This was followed by a more or less linear decrease to near 20% near the end of the run. The time average selectivity was, as shown earlier, about 55%.

Maximum selectivity to elemental sulfur occurred at low temperature, small regeneration gas flow rate, and large H_2O-to-O_2 ratio. Complete regeneration could not be achieved below about 600°C; at 550°C, used in run FeS-04, regeneration was incomplete, presumably because of the formation of $Fe_2(SO_4)_3$ and/or $Al_2(SO_4)_3$. However, as shown from the sulfur material balance results of FeS-22, there was no indication of $Fe_2(SO_4)_3$ formation at higher temperatures.

Concentration-time results from test FeS-19 at 700°C are shown in Fig. 8. Regeneration conditions other than temperature were identical in runs FeS-19 and FeS-22. The general concentration-time responses were similar as were the total run duration, maximum concentration of total sulfur, and the time corresponding to the total sulfur maximum. However, the maximum SO_2 concentration was about 50% larger at the higher temperature and the maximum occurred at an earlier time. The largest differences were associated with the H_2S where maximum concentration was doubled and the time corresponding to the maximum was reduced by about 25%. Only about 40% of the sulfur released in run FeS-19 was in elemental form, compared to 55% in run FeS-22.

Doubling the regeneration gas feed rate from 300 sccm in run FeS-22 to 600 sccm in FeS-26, while keeping other regeneration conditions constant, produced a moderate negative effect on the production of elemental sulfur. The H_2S and SO_2 responses with time were qualitatively similar to those shown in Fig. 5 and 8, but the maxima were at larger mol fractions. Slightly less than 50% of the sulfur was liberated in elemental form in FeS-26 compared to

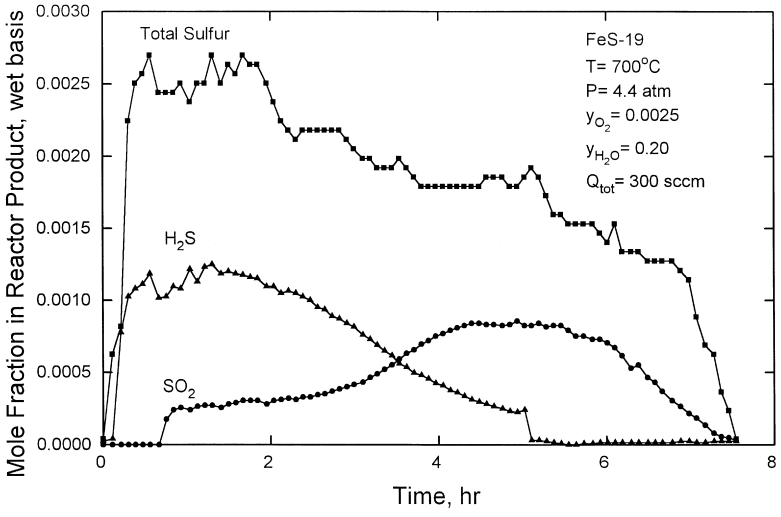

Fig. 8. Concentrations of sulfur species during steam-oxygen regeneration at high temperature: run FeS-19.

55% in FeS-22. We attribute the decrease in elemental sulfur production to reduced contact time for the Claus reaction at the larger feed rate.

Varying the H_2O-to-O_2 ratio produced the largest effect on elemental sulfur production. This may be seen from the concentration-time results of run FeS-16 using H_2O-to-O_2 ratio of 6.7 shown in Fig. 9. The sum of the H_2S and SO_2 concentrations was approximately equal to the total sulfur concentration, indicating that the amount of elemental sulfur was quite small. Although the higher temperature and larger feed rate in FeS-16 also contributed to reduced elemental sulfur formation, these effects were not sufficient to explain the almost total absence of elemental sulfur.

The maximum elemental sulfur yield was achieved in run FeS-25 where approximately 75% of the sulfur was liberated in elemental form using a H_2O-to-O_2 ratio of 200. Time-concentration results for this run are shown in Fig. 10. Although the total feed rate in FeS-25 was somewhat higher than in FeS-22, the

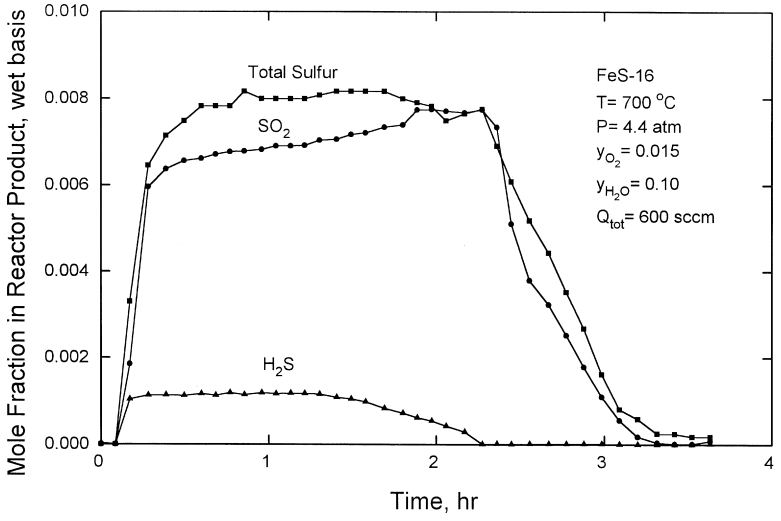

Fig. 9. Concentrations of sulfur species during steam-oxygen regeneration using small steam-to-oxygen ratio: run FeS-16.

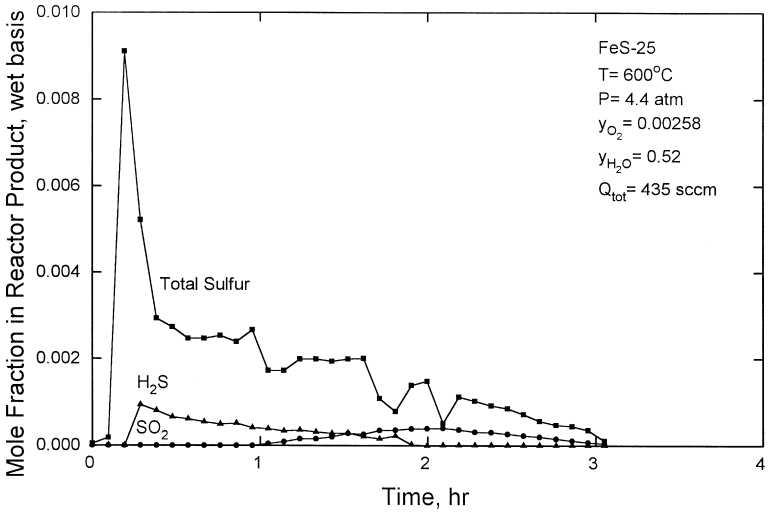

Fig. 10. Concentrations of sulfur species during steam-oxygen regeneration using large steam-to-oxygen ratio: run FeS-25.

larger feed rate should, based on previous discussion, slightly reduce the elemental sulfur yield. With the exception of the very large early peak in total sulfur concentration, the results in Fig. 10 are qualitatively similar to results presented earlier. However, the cumulative yields of H_2S and SO_2 were only 15% and 10% of theoretical, respectively, and about 75% of the sulfur was produced in elemental form.

4. Discussion

The experimental results may be interpreted qualitatively on the basis of reactions (R1) through (R4). Conceptual solid and gas concentration profiles within the sorbent bed during early stages of the reaction are shown in Fig. 11. Since the FeS–O_2 reaction is quite fast, the reaction interface separating Fe_2O_3 and FeS is quite steep. The reaction between FeS and H_2O is relatively slow, and the Fe_3O_4–FeS interface is indicated by the almost horizontal line. In addition, Fe_3O_4 will exist only downstream of the Fe_2O_3–FeS interface since it will be quickly converted to Fe_2O_3 when contacted by O_2.

The O_2 concentration profile at any time is approximately equivalent to the Fe_2O_3–FeS interface, but distorted due to the consumption of oxygen in converting Fe_3O_4 to Fe_2O_3. No H_2O reacts upstream of the Fe_2O_3–FeS interface, and the H_2O concentration

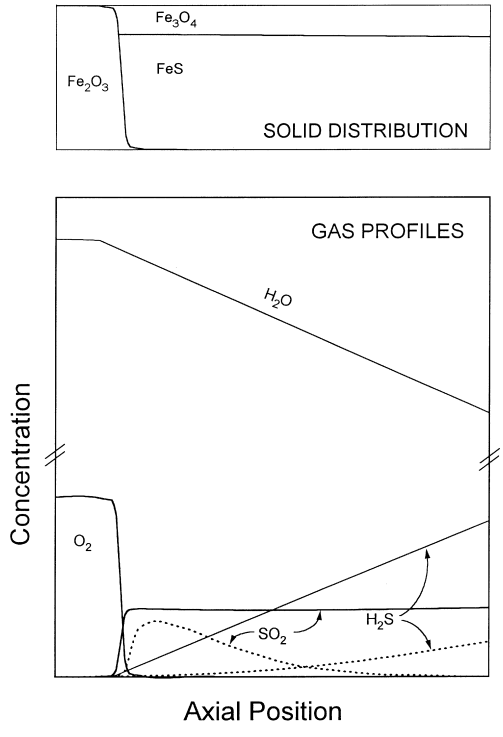

Fig. 11. Solids distribution and gas concentration profiles within the sorbent bed at an early stage of the reaction.

profile downstream of the Fe_2O_3–FeS interface is almost horizontal, similar to the Fe_3O_4–FeS interface. Note that the concentration axis in Fig. 11 is discon-

tinuous and H_2O concentration is much greater than O_2 concentration. Although there appears to be a significant change in H_2O concentration, in reality the percentage change is quite small.

In the absence of the Claus reaction, the SO_2 concentration profile is quite steep. The H_2S concentration is zero to the Fe_2O_3–FeS interface and increases almost linearly from there to the exit of the sorbent bed. These profiles are shown by the solid lines in Fig. 11. When SO_2 and H_2S co-exist, elemental sulfur is formed by the Claus reaction and the SO_2 and H_2S concentration profiles are modified as shown by the dashed lines. No additional SO_2 is formed downstream of the Fe_2O_3–FeS interface, which means that the SO_2 concentration reaches a maximum at some interior bed position and decreases therafter. In contrast, all of the H_2S is formed downstream of the Fe_2O_3–FeS interface, and additional H_2S is formed downstream of the point where SO_2 concentration is zero.

The amount of SO_2 formed is relatively independent of time until O_2 breakthrough occurs, after which the amount of SO_2 formed decreases. The major difference is the axial position of the reaction interface. In contrast, the amount of H_2S produced is a maximum during the initial stages of the reaction and decreases continuously with time. The maximum amount of H_2S coupled with the maximum contact time between H_2S and SO_2 explains why the elemental sulfur selectivity is maximum initially and decreases with time. Similarly, the fixed quantity of SO_2 comes in contact with the maximum amount of H_2S for the maximum amount of time at the early stages of the reaction. All of the SO_2 reacts leading to zero SO_2 product gas concentration.

Solid and gas concentration profiles at an intermediate reaction time are sketched in Fig. 12. The shape of the Fe_2O_3–FeS interface is similar to the profile at the earlier time, but displaced to the right. No Fe_3O_4 exists upstream of the Fe_2O_3–FeS interface. The Fe_3O_4–FeS interface remains almost flat but the Fe_3O_4 concentration is increased due to the longer reaction time. The O_2 concentration profile is similar to the earlier profile, but also displaced downstream. The H_2O profile remains flat but even less H_2O reacts because of the reduced contact time downstream of the Fe_2O_3–FeS interface. In the absence of the Claus reaction (solid lines) the SO_2 profile is unchanged

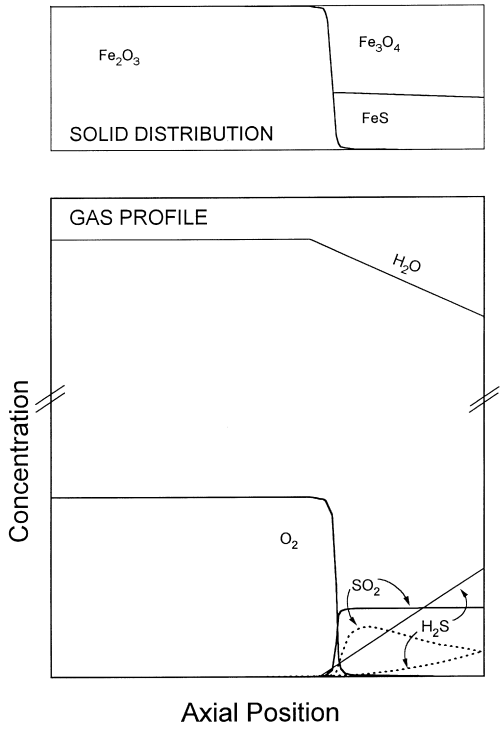

Fig. 12. Solids distribution and gas concentration profiles within the sorbent bed at an intermediate stage of the reaction.

except for the downstream position. The H_2S concentration profile is similar but at a lower concentration level than at earlier time. When the Claus reaction is considered (dashed lines), less SO_2 is consumed because less H_2S is present and the contact time is less; therefore, both SO_2 and H_2S appear in the product gas.

The effects of flow rate, temperature and H_2O-to-O_2 ratio on elemental sulfur production described in the experimental results section are consistent with the above description. Doubling the feed gas rate from 300 to 600 sccm (runs FeS-22 and FeS-26) increased the selectivity to SO_2, had little effect on the H_2S selectivity, and, as a consequence, reduced the elemental sulfur selectivity. The increased flow rate caused no change in the SO_2 production rate. However, less H_2S was formed due to the reduced residence time, and there was less time for the Claus reaction to occur. These effects tend to cancel with respect to H_2S production, but result in greater SO_2 selectivity and reduced elemental sulfur yield.

Higher temperature, in contrast, increased the H_2S yield, had little effect on the amount of SO_2 produced, and caused the elemental sulfur selectivity to decrease. Independent studies [14] have shown that the FeS–H_2O reaction is more sensitive to temperature than the FeS–O_2 reaction. Therefore, higher temperature increased the amount of H_2S formed while having little effect on SO_2 production. However, much of the H_2S was formed downstream of the main FeS–Fe_2O_3 reaction front and had less opportunity to react with SO_2.

The strong effect of the H_2O-to-O_2 ratio on elemental sulfur selectivity, which ranged from almost zero at a ratio of 6.7 (run FeS-16) to about 75% at a ratio of 200 (run FeS-25), is also due to the large difference in the intrinsic reaction rates of FeS with O_2 and H_2O. Large selectivity to elemental sulfur requires that a large fraction of the FeS be converted to H_2S, and, of equal importance, that both SO_2 and H_2S be formed at positions within the bed which provide sufficient time for the Claus reaction to occur. H_2S formed near the exit of the sorbent bed is swept out of the reactor without having the chance to be converted to elemental sulfur.

Acknowledgements

The authors their gratitude to the U.S. Department of Energy, Federal Energy Technology Center for financial support under contract DE-RP21-94MC30012, and to Thomas P. Dorchak of FETC for his advice and support on technical matters.

References

[1] A.L. Kohl, F.C. Riesenfeld, Gas purification, Gulf publishing, Houston, 1979, p. 28.

[2] P.W. Sage, World energy resources, their use and the environment, paper presented at the NATO advanced studies institute on desulfurization of hot coal gas with regenerable metal oxide sorbents, Kusadasi, Turkey, July 1996 (proceedings to be published).

[3] T. Grindley, G. Steinfeld, Testing of zinc ferrite hydrogen sulfide sorbent in a coal gasifier sidestream, Proc. 4th Ann. Meeting on Contaminant Control in Hot Coal-Derived Gas Streams, Morgantown WV, December 1984, DOE/METC-85/3 p. 314.

[4] G.D. Focht, P.V. Ranade, D.P. Harrison, High temperature desulfurization using zinc ferrite: reduction and sulfidation kinetics, Chem. Eng. Sci. 43 (1988) 3005.

[5] S. Lew, K. Jothimurugesan, M. Flytzani-Stephanopoulos, High temperature hydrogen sulfide removal from fuel gas by regenerable zinc oxide–titanium dioxide sorbents, Ind. Eng. Chem. Res. 28 (1989) 535.

[6] M.C. Woods, S.K. Gangwal, K. Jothimurugesan, D.P. Harrision, The reaction between H_2S and zinc oxide–titanium oxide sorbents: single pellet kinetic studies, Ind. Eng. Chem. Res. 30 (1990) 1160.

[7] S.K. Gangwal, Enhanced durability of desulfurization sorbents for fluridized-bed applications, Proc. 10th Ann. Gasification and Gas Stream Systems Review Meeting, Morgantown, WV, August 1990, DOE/METC-90/6115 (DE90009689) p. 102.

[8] U.S. Department of Energy, Clean Coal Technology Demonstration Program-Program Update 1994, DOE/F3-0030, 1995.

[9] D.P. Harrison, Performance analysis of ZnO-based sorbents in removal of H_2S from fuel gas, paper presented at the NATO advanced studies institute on desulfurization of hot coal gas with regenerable metal oxide sorbents, Kusadasi, Turkey, July 1996 (proceedings to be published).

[10] A.G.J. van der Ham, Regenerative high temperature desulfurization of coal gas in a circulating fluidized bed, Ph.D. Thesis, University of Twente, The Netherlands, 1994.

[11] T. Grindley, G. Steinfeld, Development and testing of regenerable gas desulfurization sorbents, DOE/MC/16545-1125, 1981.

[12] H.A. Bennett, A. Meisen, Experimental determination of air–H_2S equilibria under Claus furnace conditions, Can. J. Chem. Eng. 59 (1981) 532.

[13] W.J. McMichael, S.K. Gangwal, recovery of sulfur from hot gas desulfurization process, DE-AC21-86MC23260, 1991.

[14] W. Huang, Regeneration of iron sulfide with oxygen, steam, and oxygen–steam mixtures, M.S. Thesis, Louisiana State University, May 1997.